DTM REFINEMENT USING MULTI IMAGE SHAPE FROM SHADING

C. Piechullek, C. Heipke

Technical University Munich
Chair for Photogrammetry and Remote Sensing
Munich, Germany
E-Mail: peik@photo.verm.tu-muenchen.de

Working Group III/2: Geometric-Radiometric Models and Object Reconstruction

KEY WORDS: Shape from Shading, radiometric surface model, DTM reconstruction, simulation

ABSTRACT

We present a new approach to Shape from Shading (SFS) to be used with imagery of the MARS96 HRSC/WAOSS mission. The work builds upon prior investigations of multi image SFS [Heipke 1992; Heipke, Piechullek 1994]. Our SFS approach simultaneously processes multiple images and incorporates an object space model for the terrain surface. In contrast to most SFS methods which rely on the often too simple Lambertian surface reflection we introduce the Lommel-Seeliger law widely used in planetary science [Lumme, Bowell 1981; Hapke 1993] for modeling light reflection at the object surface. We investigate both the Lambertian and the Lommel-Seeliger model using synthetic images in order to compare the characteristics of both approaches and to show the advantages over existing SFS methods.

1. INTRODUCTION

Shape from Shading (SFS) is a technique for surface reconstruction which exploits the fact that surface patches, having different orientation towards a light source, are imaged with different brightness in the images. The grey values of these patches are directly related to surface inclination. The surface is generally assumed to have uniform reflectance properties. Therefore, SFS only performs well in areas with poor image texture.

Digital image matching is a widely used tool in digital photogrammetry to derive surface information from multiple images. In the absence of sufficient, non-periodic image texture, however, digital image matching techniques fail to produce correct and reliable results. Thus, SFS can be used as a means to complete and refine a digital terrain model (DTM) which has been generated by digital image matching.

The basic assumption for all SFS algorithms states that since different parts of a surface have different orientations relative to the direction of illumination they are imaged with different brightness. This spatial variation in brightness, called shading, is used to locally reconstruct the surface slope. The surface is described by small planar surface elements; the size of a surface element approximately equals the size of a pixel multiplied with the average image scale factor. The inclinations of neighbouring surface elements are then integrated to produce a geometric model of the object surface; all other influences which take part in the image formation process, i.e. illumination, sensor or atmosphere are assumed to be known.

The basic equation of SFS can be derived assuming a constant albedo A along with Lambertian reflectance for the whole surface. In this case, the grey value g(x',y') at the position x', y' in image space only depends on the angles between illumination direction, viewing direction and the local surface normal. Since the local normal vector $\mathbf{n} = [-n_X;-n_Y;1]^T$ contains two unknown components for surface inclination, namely n_X and n_Y, but only one observation, namely g(x',y'), for each point in object space, there exists an infinite number of inclinations, which all result in the same grey value. To overcome this indeterminability, additional information must be brought to bear. For possible solutions and a detailed bibliography on SFS see [Horn, Brooks 1989].

2. IMAGE FORMATION

In this chapter the image formation process is shortly reviewed, since the relation between surface reflectance properties and image irradiance is the basis for our SFS model.

Trying to express the orientations of the surface patches as a function of the grey values makes it necessary to take into account all influences in object and image space which are part of the imaging process. The amount of radiance reflected towards a sensor is a function of

- the illumination direction **s**,
- the viewing direction **v** and
- the orientation **n** of the local surface normal.

These directions enclose
- the incidence angle *i*;
- the emittance angle *e*;
- the phase angle *g* (see figure 1).

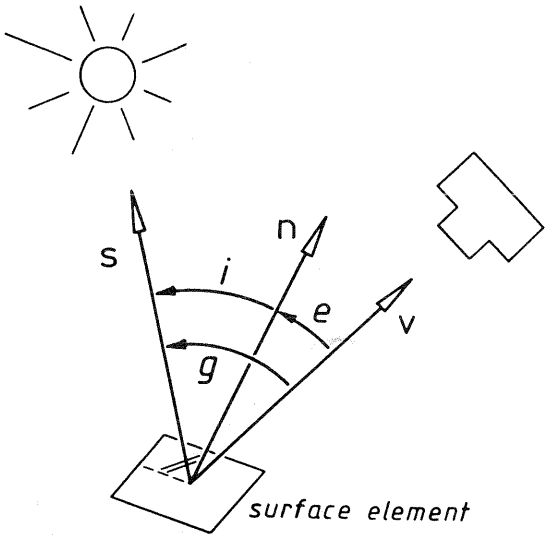

Figure 1: Imaging geometry

Besides these geometrical relations, the image grey values are influenced by
- illumination (radiance and wavelength of the incident radiation; distance and extension of the source);
- atmosphere (absorption, transmission, refraction);
- sensor (radiometric sensitivity of the opto-electronic components; interior and exterior orientation);
- surface (light reflectance properties of the surface layer).

In the investigated approach, the light source is introduced as a distant point light source with known radiometric characteristics. Atmospheric influences are considered to be neglectible, while the sensor parameters are assumed to be known by radiometric and geometric calibration.

Next two radiometric models are presented which serve to describe the reflectance properties of planetary surfaces. Besides the well-known Lambert law the Lommel-Seeliger law is derived in more detail.

In the field of planetary photometry a series of models for the description of light scattering on planetary surfaces were developed [Minnaert 1941; Hapke 1981; Lumme, Bowell 1981; McEwen 1991]. While photometry aims at the derivation of parameters describing geological state and situation of planetary regoliths, SFS tries to relate observed brightnesses to the angles *i*, *e* and *g* and thus surface topography, along with surface reflectance (or albedo).

In both models, light with irradiance E_0 which is assumed to be collimated, falls on a surface layer, enclosing the incidence angle *i* between local surface normal and the direction to the light source. The irradiance is partly absorbed and partly scattered back into the upper hemisphere. A sensor lying in direction **v**, which encloses the emittance angle *e* between viewing direction and local surface normal registers the incoming radiance $L_e(i,e,g)$.

To describe this direction-dependent reflectance the so-called bidirectional reflectance (BDR) $r(i,e,g)$ is defined as the ratio between radiance $L_e(i,e,g)$ scattered towards the sensor, and the incoming surface irradiance E_0:

$$r(i,e,g) = L_e(i,e,g) / E_0 \qquad (1)$$

The relation between the BDR and other quantities related to reflectance (e.g. the bidirectional reflectance distribution function (BRDF)) is given by [Hapke 1993].

The Lambert law of reflectance is based on the assumption that the brightness of a surface depends only on the incidence angle *i* and is independent of the emittance angle *e*, i.e. the surface looks equally bright from every viewing direction. Consequently, the scattered radiance $L_e(i,e,g)$ has to be proportional to E_0 per unit surface area. The BDR for a Lambert surface is

$$r(i) = A_L \cdot \cos i \qquad (2)$$

A_L (Lambert albedo) is a constant which describes the ratio between reflected radiance and incoming irradiance per unit surface area. The Lambert law is widely used in SFS algorithms for its simplicity, though no natural surface strictly obeys it. Especially for low-albedo surfaces, such as rocky planetary bodies, the assumption of Lambertian reflectance is not valid.

In order to derive a more general photometric function, a model for the reflection of electromagnetic radiation is presented which describes light scattering within a semiinfinite, particulate medium which scatters light only once. This model is known as the Lommel-Seeliger law and was first described by Seeliger in 1887. It extends the assumption that light reflection occurs at the boundary surface between two media only. Instead, light scattering is assumed to be a phenomenon which takes place at individual particles within a layer of infinite thickness below the apparent surface; the radiance observed at a sensor comes from light scattered by all particles in the medium that lie within the field of view of the sensor. an exhaustive treatment of this topic can be found in [Hapke 1993]; a short derivation of the Lommel-Seeliger law follows.

A horizontally extended surface layer of infinite thickness consists of scattering particles with mean scattering cross-section c_s and (constant) particle density ρ_p. Now consider a layer of thickness dZ in depth Z within the medium. This layer is illuminated by light with irradiance E_0 under angle *i* (see figure 2).

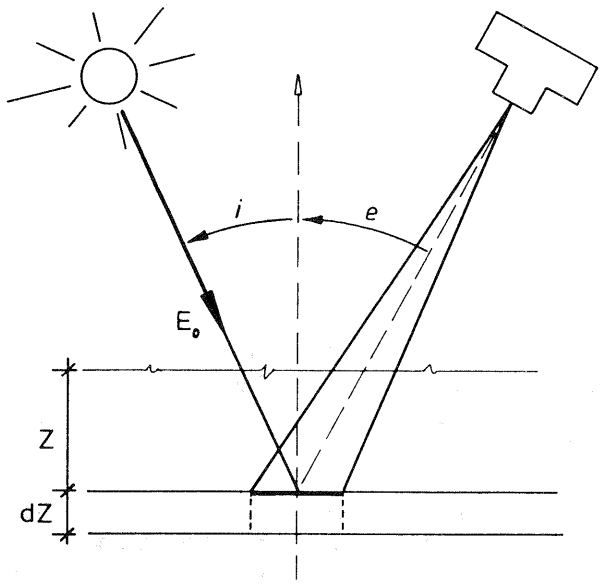

Figure 2: Derivation of the Lommel-Seeliger law

The probabilities for a photon to enter the layer and to emerge again towards the sensor can be described by two exponential attenuation factors:

$$p_i(Z) = e^{\frac{-\tau}{\cos i}} \quad ; \quad p_e(Z) = e^{\frac{-\tau}{\cos e}} \qquad (3)$$

The optical depth τ is a means to describe how far incident radiation will penetrate into the medium. It is defined as

$$\tau = \int_{Z'=Z}^{\infty} \rho_p c_s dZ' \;\Rightarrow\; d\tau = -\rho_p c_s dZ \qquad (4)$$

The amount of radiation that 1) travels through the surface to depth Z, interacting with the particles within the layer, and 2) is scattered towards the sensor after attenuation by the particles lying above the layer is given by

$$dL(Z) = -E_0 R \cdot p_i(Z) \cdot p_e(Z) \frac{d\tau}{\cos e} \qquad (5)$$

The factor R denotes the amount of light that is scattered towards the direction of the sensor by a single particle. R depends on the particle's scattering behaviour; if the particles within the surface layer are considered to be isotropic scatterers, i.e. if they scatter incident radiation equally in all directions, R can be replaced by the so-called single-particle scattering albedo w; the factor $1/4\pi$ is introduced for normalization purposes, [Hapke 1993]. The total amount of radiance that is scattered towards the sensor is obtained by integration over all layers:

$$\begin{aligned} L_e(i,e) &= E_0 \frac{w}{4\pi} \int_{\tau=0}^{\infty} e^{\frac{-\tau}{\cos i}} e^{\frac{-\tau}{\cos e}} \frac{d\tau}{\cos e} \\ &= E_0 \frac{w}{4\pi} \cdot \frac{\cos i}{\cos i + \cos e} \end{aligned} \qquad (6)$$

Substituting equation (6) into equation (1) leads to the Lommel-Seeliger law:

$$r(i,e) = \frac{w}{4\pi} \cdot \frac{\cos i}{\cos i + \cos e} \qquad (7)$$

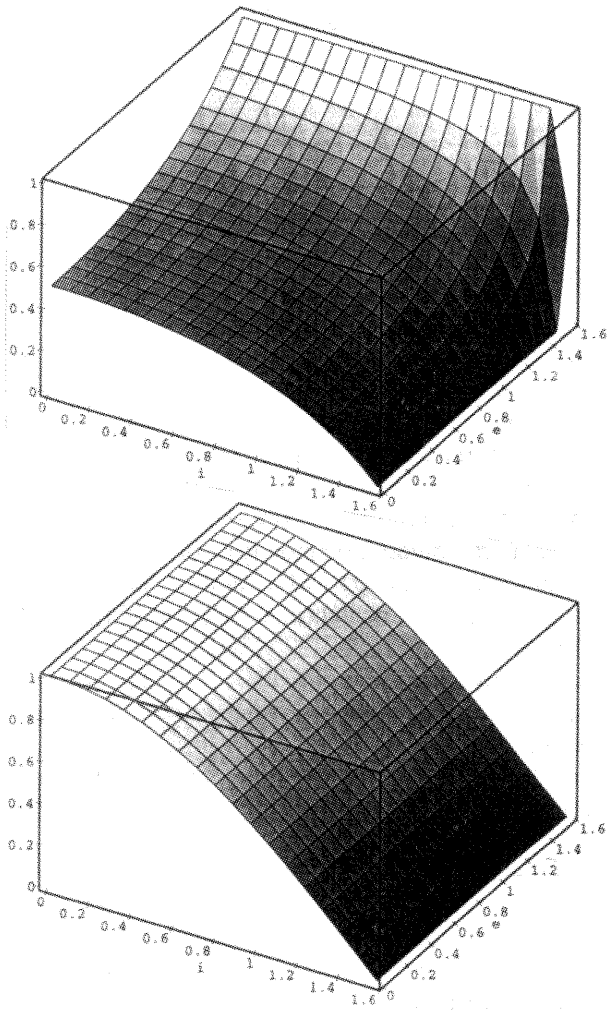

Figure 3: The Lommel-Seeliger law (top) in comparison to the Lambert law (bottom)

This photometric function is a good description of the light scattering behaviour of low-albedo surfaces, [McEwen 1991, Hapke 1993], in contrast to the Lambert law, which is more valid for bright surfaces. Some of the most sophisticated reflectance models

widely used in planetary photometry, e.g. [Lumme, Bowell 1981; Hapke 1981, 1984, 1986, 1993], are extensions of the Lommel-Seeliger law. Hence, this model can be used to describe the reflectance properties of planetary surfaces, assigning a constant, known single-particle scattering albedo w to the whole surface.

Figure 3 shows the Lommel-Seeliger law in comparison to the Lambert law. The significant increase in brightness for large emittance angles e is due to the fact that with increasing e the area of the imaged surface layer also increases by $1/\cos e$, and thus a greater part of the surface layer contributes to the brightness observed in the sensor.

The connection between the image grey values g(x',y') and the reflected radiance L_e is given by substituting equation (7) into the camera equation, [Horn 1986],

$$\begin{aligned} g(x',y') &= k \cdot E_i(x',y') \\ &= k \cdot \frac{\pi d^2 \cos^4\gamma}{4f^2} \cdot E_0 \cdot r(i,e,g) \end{aligned} \tag{8}$$

E_i image irradiance
d diameter of the optical lens
f focal length of the sensor
γ angle between optical axis and image ray
k rescaling constant

combining all terms, which are independent of i and e into the reflectance coefficient A_R:

$$g(x',y') = A_R(w) \cdot \frac{\cos i}{\cos i + \cos e} \tag{9}$$

3. MULTI IMAGE SHAPE FROM SHADING

Multi-image Shape from Shading has been introduced by [Heipke 1992; Heipke, Piechullek 1994]. It uses at least two images simultaneously to determine the heights of a predefined geometric object model. The grey values of the images are directly related to the unknown heights of a DTM which is defined in object space. The main characteristics of the method are:

- perspective transformation from object space to image space;
- no need for corresponding points, since neighbouring surface elements are assumed to have the same albedo;
- least-squares estimation of the unknowns;
- high accuracy potential.

In the quoted references, the Lambertian reflectance model was used to describe the reflectance properties for the imaged surface, leading to the following non-linear observation equation per pixel per image:

$$v = A_R \cos i(\hat{Z}_i) - g(x'(\hat{Z}_i), y'(\hat{Z}_i)) \tag{10}$$

v least squares residual of observation equation
$\hat{Z}_i$ unknown heights of the geometric surface model

In this paper two extensions are presented. First, we have incorporated the Lommel-Seeliger law as photometric function for the surface. Second, the reflectance coefficient A_R (and thus the albedo of the surface) is also considered unknown, and is estimated together with the unknown surface heights. The corresponding non-linear observation equation reads:

$$\begin{aligned} v = \hat{A}_R \frac{\cos i(\hat{Z}_i)}{\cos i(\hat{Z}_i) + \cos e(\hat{Z}_i)} \\ - g(x'(\hat{Z}_i), y'(\hat{Z}_i)) \end{aligned} \tag{11}$$

After linearization of the observation equations (10) and (11), respectively, the unknowns $\hat{Z}_i$ and $\hat{A}_R$ are estimated in an iterative least-squares adjustment.

4. EXPERIMENTS AND RESULTS

Some experiments on surface reconstruction using the Lambert and the Lommel-Seeliger law with varying initial information for the unknown surface parameters are presented in this chapter in order to evaluate the potential of both approaches. All experiments have been conducted using synthetic images which approximate the imaging geometry of the HRSC camera, [Albertz et al. 1993], when imaging near the closest approach to the Martian surface.

4.1. Input data

To generate the synthetic images, a continuous, hilly terrain with an area of 4940*4940 m^2 and a maximum height difference of about 1550 m was approximated by a DTM of 26*26 meshes with a mesh size of 190*190 m^2 each (see figure 4).

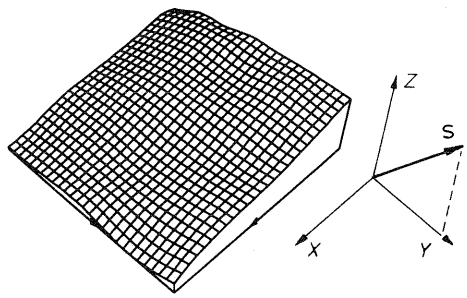

Figure 4: Reference DTM for the generation of the images

From this DTM two shaded relief images were generated using 1) the Lambert and 2) the Lommel-

Seeliger law as a model for the surface reflectance properties, along with a distant point light source with known irradiance E_0 and known illumination direction. Each DTM mesh was divided into 10*10 object surface elements with constant albedo. Each of these shaded relief images was then projected into the different images with known exterior orientation parameters by using a ray tracing algorithm.

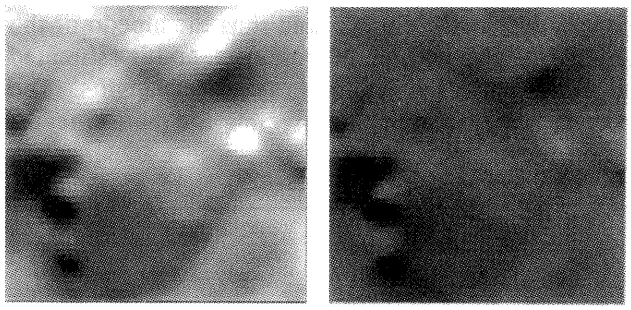

Figure 5: The same surface, shaded with the Lambertian (left) and the Lommel-Seeliger (right) photometric function

Figure 5 shows the same surface as it is imaged from the same camera position, but with the two different surface reflectance functions. To approximate the imaging geometry of the HRSC camera near the closest approach to the Martian surface, the orientation parameters of the images were defined as follows (see figure 6):

- three images on a straight line with a base length of 163 km between neighbouring images;
- flight altitude: 475 km;
- stereo angle: 19°;
- object surface element size (ground resolution): 19*19 m^2.

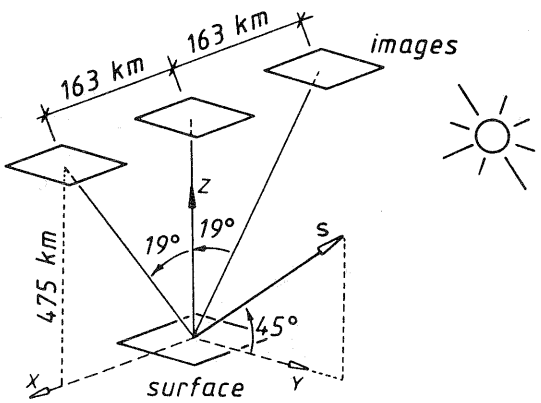

Figure 6: Setup for the generation of the images

These images, along with known exterior orientation parameters and different initial values for the unknowns, were introduced to our algorithm in order to reconstruct the DTM heights and the surface albedo.

4.2. Conducted experiments

Four groups of experiments were conducted using the three images for each simulation. All experiments were stopped when the changes to the unknown heights and the albedo from one iteration to the next fell below a predefined threshold of 1 m for the heights and 1 grey value for the albedo, respectively. The following experiments were conducted:

1) Surface reconstruction with known, error-free albedo and a horizontal plane as initial DTM. This experiment was carried out with the Lambert and the Lommel-Seeliger model.
2) Surface reconstruction with known, error-free heights and a known, error-free albedo which is 5% smaller than the correct value (only performed with the Lommel-Seeliger model);
3) Reconstruction of a Lambert surface with the Lommel-Seeliger model.
4) Surface reconstruction with the Lommel-Seeliger model, introducing a horizontal plane as initial height information, along with a wrong and unknown albedo. This experiment has been conducted with an albedo value which is 5%, 10%, 15%, 20% and 50% smaller than the correct one which was used to generate the input images.

4.3. Results

All simulations show that the relative height differences between neighbouring surface elements can be computed after a few iterations; the absolute height offset of the whole surface is reconstructed more slowly. Changing the orientation of a surface element immediately changes its grey value (see equations (10) and (11)); a change of the absolute height offset causes the whole image of the surface to be shifted in image space, without changing the grey value differences between neighbouring surface elements to a large extent. As for the four groups of experiments, the following results were achieved:

- Introducing a horizontal plane as initial height information, along with known and error-free albedo allows for a correct reconstruction of the Lommel-Seeliger surface; remaining height differences ΔZ between the correct DTM and the result of the surface reconstruction are in the order of $\Delta Z/h \approx 10^{-6}$ and are caused by quantisation errors during the generation of the images. In the Lambert case, however, the surface is reconstructed incorrectly; while the surface inclinations in the vertical plane containing the light source direction s are correct, the inclinations perpendicular to this plane are wrong, causing a 'profiling' of the surface. Figure 7 shows the reconstructed surface (left), along with the differences between correct and reconstructed heights (right); s denotes the illumination direction. Since the Lambert photometric function is

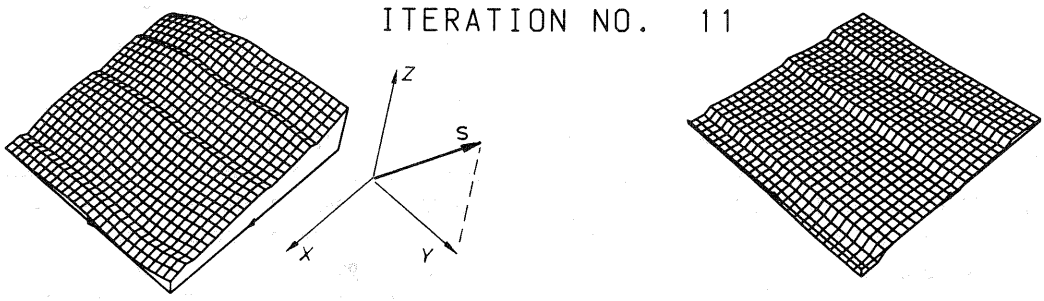

Figure 7: Result of the surface reconstruction with the Lambert model (A_R known, error-free; horizontal plane as initial DTM)

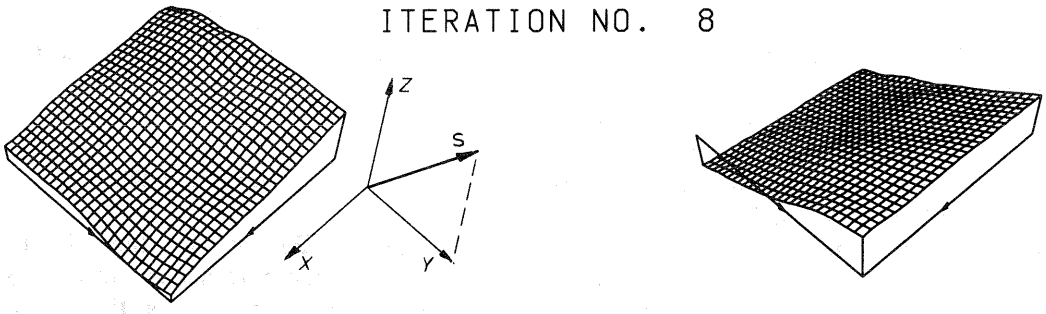

Figure 8: Result of the surface reconstruction with the Lommel-Seeliger model (wrong, error-free A_R; horizontal plane as initial DTM)

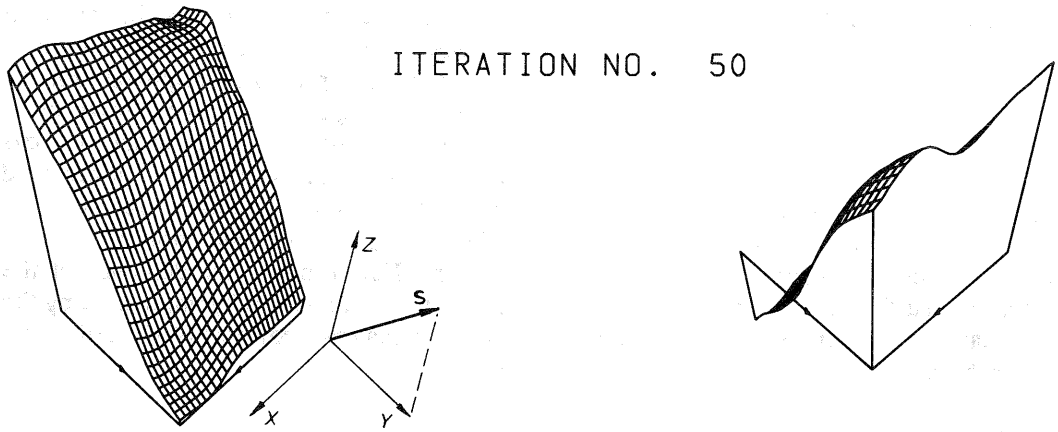

Figure 9: Result of the surface reconstruction with the Lommel-Seeliger model, if a Lambert surface is introduced

independent of viewpoint, the three images of the surface are equal, except for different perspective distortions. Consequently, the additional images do not contribute additional information to the estimation of the surface inclinations perpendicular to the mentioned plane - this is in line with the general indeterminability of classical SFS (see introduction).

- The reconstruction of a surface with error-free heights and a wrong, error-free albedo which is 5% lower than the correct one causes the whole surface to be tilted towards the illumination direction, because all grey values which are computed from the initial values are a constant factor smaller than the image grey values. This effect is nearly independent of the surface topography, as can be seen from the differences between reference DTM and reconstructed DTM (see figure 8); the height differences between neighbouring DTM heights are nearly constant. All grey value differences are interpreted as resulting from an incorrect angle between local surface normal and illumination direction s.
- The reconstruction of a Lambertian surface by the Lommel-Seeliger approach causes the whole surface to be tilted extremely away from the viewing direction, since large grey values in the Lommel-Seeliger law are directly related to large emittance angles e (see figure 9). In contrast to the simulation with wrong, error-free albedo, there is also an influence of surface topography on the differences

between reference DTM and reconstructed DTM. While in simulation 2) the difference between observed and calculated grey value is due to a constant factor, in this simulation the difference is caused by a wrong assumption concerning the relation between the grey values and the angles *i* and *e*. It should be noted that in this case a large number of iterations had to be performed before a convergence was reached.

- The last group of simulations served to assess, whether unknown albedo can be estimated together with unknown DTM heights. The DTM heights could be successfully reconstructed in all experiments. The unknown albedo nearly reached the correct value after the first iteration. The remaining height offset and surface tilt are then removed, until the correct values for the heights and the albedo are achieved. In comparison to simulation 2), where a wrong albedo caused a tilt of the whole surface towards the light source, the grey value differences here result in an improvement of the albedo in order to remove this tilt. This is due to the fact that the albedo is a constant factor, which influences all grey value observations in the same way. Since this behaviour is independent of the difference between correct and initial albedo value, all experiments reconstructed the surface heights and the albedo after the same (few) number of iterations.

4.4. Conclusions

Our SFS algorithm has been tested successfully using synthetic images. In comparison to the well-known Lambert law, the Lommel-Seeliger law was introduced, along with unknown surface albedo, as a model for the surface reflectance properties. The following conclusions can be drawn from the results presented above:

- The Lambert law turns out to be unstable, resulting in singularities for the surface reconstruction, if multiple images with identical illumination direction are introduced. This behaviour is independent of the exterior orientation of the images, since the image grey values are not influenced by the camera position;
- The Lommel-Seeliger law allows for a correct surface reconstruction, even if all images are introduced with identical illumination direction. The image grey values are a function of camera position, and therefore additional independent information is available for the surface reconstruction;
- SFS using the Lommel-Seeliger law is a method to reconstruct unknown heights correctly, even if poor initial values, e.g. a horizontal plane, are introduced;
- Unknown albedo can be estimated correctly from the images, along with unknown heights, even if an extremely wrong initial albedo value is introduced; this is due to the fact that the initial value for the albedo affects all grey value observations in the same way.
- Wrong albedo introduced as error-free results in an incorrect inclination of the whole surface relative to the illumination direction. The relative height differences within the surface, however, can be reconstructed with high accuracy;
- If the imaged surface does not obey the modeled reflectance behaviour, completely wrong heights are obtained. In contrast to a surface reconstruction with wrong albedo, the resulting height differences are also a function of the surface topography. Therefore, SFS can only produce correct results, if the reflectance properties of the surface are modeled appropriately.

5. OUTLOOK

Multi-image SFS using the Lommel-Seeliger photometric function turned out to yield good results, even if poor initial values for the unknown surface parameters are available only. Additionally, this approach can overcome singularities which occur when Lambert surfaces have to be reconstructed from multiple images with identical illumination direction. However, only synthetic images have been used; therefore, the presented approach has to be tested using real imagery of poorly textured surfaces, such as planets or asteroids, in order to evaluate the correctness of the surface reflectance model, and to assess the robustness and reliability of the methods when image noise and non-uniform albedo are present. Furthermore, the demands of the MARS96 mission have to be met by implementing the three-line scanner imaging geometry of the HRSC and WAOSS sensors.

6. REFERENCES

Albertz J., Scholten F., Ebner H., Heipke C., Neukum G. (1993): Two Camera Experiments on the Mars 94/96 Mission. GIS 6 (4), 11-16

Hapke B. (1981): Bidirectional Reflectance Spectroscopy; 1. Theory. Journal of Geophysical Research 86 (B4), 3039-3054

Hapke B. (1984): Bidirectional Reflectance Spectroscopy; 3. Correction for Macroscopic Roughness. Icarus 59, 41-59

Hapke B. (1986): Bidirectional Reflectance Spectroscopy; 4. Extinction and the Opposition Effect. Icarus 67, 264-280

Hapke B. (1993): Theory of Reflectance and Emittance Spectroscopy. Topics in Remote Sensing III. Cambridge University Press

Heipke C. (1992): Integration of Digital Image Matching and Multi Image Shape from Shading, in: Mustererkennung 1993, 15. DAGM-Symposium, Pöppl S.J., H. Handels (eds.). Informatik aktuell, Springer, Berlin, 367-374

Heipke C., Piechullek C. (1994): Towards Surface Reconstruction Using Multi Image Shape from Shading. IntArchPhRS (30) 3/1, 361-369

Horn B.K.P. (1986): Robot Vision. The MIT Press, Cambridge

Horn B.K.P., Brooks M.J. (eds.) (1989): Shape from Shading. The MIT Press, Cambridge

Lumme K., Bowell E. (1981): Radiative Transfer in the Surfaces of Atmosphereless Bodies; I. Theory. Astronomical Journal 86, 1694-1704

McEwen A.S. (1991): Photometric Functions for Photoclinometry and Other Applications. Icarus 92, 298-311

Minnaert M. (1941): The Reciprocity Principle in Lunar Photometry. Astrophysical Journal 93, 403-410